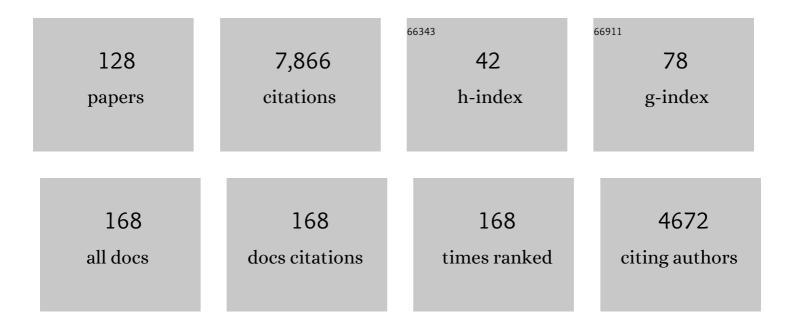
List of Publications by Year in descending order

Source: https://exaly.com/author-pdf/8825867/publications.pdf Version: 2024-02-01



#	Article	IF	CITATIONS
1	The tropospheric cycle of H <sub>2</sub> : a critical review. Tellus, Series B: Chemical and Physical Meteorology, 2022, 61, 500.	1.6	196
2	The dependence of soil H <sub>2</sub> uptake on temperature and moisture: a reanalysis of laboratory data. Tellus, Series B: Chemical and Physical Meteorology, 2022, 63, 1040.	1.6	12
3	Deposition velocity of H <sub>2</sub> : a new algorithm for its dependence on soil moisture and temperature. Tellus, Series B: Chemical and Physical Meteorology, 2022, 65, 19904.	1.6	12
4	Dry deposition of molecular hydrogen in the presence of H <sub>2</sub> production. Tellus, Series B: Chemical and Physical Meteorology, 2022, 65, 20620.	1.6	3
5	Detection of nitrous acid in the atmospheric simulation chamber SAPHIR using open-path incoherent broadband cavity-enhanced absorption spectroscopy and extractive long-path absorption photometry. Atmospheric Measurement Techniques, 2022, 15, 945-964.	3.1	3
6	Air quality observations onboard commercial and targeted Zeppelin flights in Germany – a platform for high-resolution trace-gas and aerosol measurements within the planetary boundary layer. Atmospheric Measurement Techniques, 2022, 15, 3827-3842.	3.1	1
7	Investigation of the limonene photooxidation by OH at different NO concentrations in the atmospheric simulation chamber SAPHIR (Simulation of Atmospheric PHotochemistry In a large) Tj ETQq1 1	0.78434 <b>.4</b> rgBT	/@verlock 1
8	Experimental and theoretical study on the impact of a nitrate group on the chemistry of alkoxy radicals. Physical Chemistry Chemical Physics, 2021, 23, 5474-5495.	2.8	20
9	Gas-Particle Partitioning and SOA Yields of Organonitrate Products from NO <sub>3</sub> -Initiated Oxidation of Isoprene under Varied Chemical Regimes. ACS Earth and Space Chemistry, 2021, 5, 785-800.	2.7	15
10	Characterization of a chemical modulation reactor (CMR) for the measurement of atmospheric concentrations of hydroxyl radicals with a laser-induced fluorescence instrument. Atmospheric Measurement Techniques, 2021, 14, 1851-1877.	3.1	8
11	Uptake of Waterâ€soluble Gasâ€phase Oxidation Products Drives Organic Particulate Pollution in Beijing. Geophysical Research Letters, 2021, 48, e2020GL091351.	4.0	24
12	Comparison of formaldehyde measurements by Hantzsch, CRDS and DOAS in the SAPHIR chamber. Atmospheric Measurement Techniques, 2021, 14, 4239-4253.	3.1	14
13	Highly oxygenated organic molecule (HOM) formation in the isoprene oxidation by NO <sub>3</sub> radical. Atmospheric Chemistry and Physics, 2021, 21, 9681-9704.	4.9	30
14	Atmospheric photooxidation and ozonolysis of Δ <sup>3</sup> -carene and 3-caronaldehyde: rate constants and product yields. Atmospheric Chemistry and Physics, 2021, 21, 12665-12685.	4.9	8
15	Atmospheric photo-oxidation of myrcene: OH reaction rate constant, gas-phase oxidation products and radical budgets. Atmospheric Chemistry and Physics, 2021, 21, 16067-16091.	4.9	4
16	Highly Oxygenated Organic Nitrates Formed from NO <sub>3</sub> Radical-Initiated Oxidation of β-Pinene. Environmental Science & Technology, 2021, 55, 15658-15671.	10.0	17
17	Importance of isomerization reactions for OH radical regeneration from the photo-oxidation of isoprene investigated in the atmospheric simulation chamber SAPHIR. Atmospheric Chemistry and Physics, 2020, 20, 3333-3355.	4.9	44
18	No Evidence for a Significant Impact of Heterogeneous Chemistry on Radical Concentrations in the North China Plain in Summer 2014. Environmental Science & Technology, 2020, 54, 5973-5979.	10.0	67

#	Article	IF	CITATIONS
19	Impact of NO <sub><i>x</i></sub> on secondary organic aerosolÂ(SOA) formation from <i>î±</i> -pinene and <i>l²</i> -pinene photooxidation: the role of highly oxygenated organic nitrates. Atmospheric Chemistry and Physics, 2020, 20, 10125-10147.	4.9	40
20	Evolution of NO <sub>3</sub> reactivity during the oxidation of isoprene. Atmospheric Chemistry and Physics, 2020, 20, 10459-10475.	4.9	10
21	Photooxidation of pinonaldehyde at ambient conditions investigated in the atmospheric simulation chamber SAPHIR. Atmospheric Chemistry and Physics, 2020, 20, 13701-13719.	4.9	6
22	Fast Photochemistry in Wintertime Haze: Consequences for Pollution Mitigation Strategies. Environmental Science & Technology, 2019, 53, 10676-10684.	10.0	147
23	Experimental budgets of OH, HO <sub>2</sub> , and RO <sub>2</sub> radicals and implications for ozone formation in the Pearl River Delta in China 2014. Atmospheric Chemistry and Physics, 2019, 19, 7129-7150.	4.9	92
24	Investigation of the <i>α</i> -pinene photooxidation by OH in the atmospheric simulation chamber SAPHIR. Atmospheric Chemistry and Physics, 2019, 19, 11635-11649.	4.9	17
25	Effects of NO <sub><i>x</i></sub> and SO <sub>2</sub> on the secondary organic aerosol formation from photooxidation of <i>α</i> -pinene and limonene. Atmospheric Chemistry and Physics. 2018. 18. 1611-1628.	4.9	110
26	Evaluation of OH and HO <sub>2</sub> concentrations and their budgets during photooxidation of 2-methyl-3-butene-2-ol (MBO) in the atmospheric simulation chamber SAPHIR. Atmospheric Chemistry and Physics, 2018, 18, 11409-11422.	4.9	20
27	Wintertime photochemistry in Beijing: observations of RO <sub><i>x</i></sub> radical concentrations in the North China Plain during the BEST-ONE campaign. Atmospheric Chemistry and Physics, 2018, 18, 12391-12411.	4.9	177
28	The IACOS NO <sub><i>x</i></sub> instrument – design, operation and first results from deployment aboard passenger aircraft. Atmospheric Measurement Techniques, 2018, 11, 3737-3757.	3.1	14
29	Investigation of the oxidation of methyl vinyl ketone (MVK) by OH radicals in the atmospheric simulation chamber SAPHIR. Atmospheric Chemistry and Physics, 2018, 18, 8001-8016.	4.9	22
30	Ambient and laboratory observations of organic ammonium salts in PM <sub>1</sub> . Faraday Discussions, 2017, 200, 331-351.	3.2	14
31	OH reactivity at a rural site (Wangdu) in the North China Plain: contributions from OH reactants and experimental OH budget. Atmospheric Chemistry and Physics, 2017, 17, 645-661.	4.9	63
32	Radical chemistry at a rural site (Wangdu) in the North China Plain: observation and model calculations of OH, HO <sub>2</sub> and RO <sub>2</sub> radicals. Atmospheric Chemistry and Physics, 2017, 17, 663-690.	4.9	239
33	Investigation of the <i>î²</i> -pinene photooxidation by OH in the atmosphere simulation chamber SAPHIR. Atmospheric Chemistry and Physics, 2017, 17, 6631-6650.	4.9	27
34	Comparison of OH reactivity measurements in the atmospheric simulation chamber SAPHIR. Atmospheric Measurement Techniques, 2017, 10, 4023-4053.	3.1	74
35	A new plant chamber facility, PLUS, coupled to the atmosphere simulation chamber SAPHIR. Atmospheric Measurement Techniques, 2016, 9, 1247-1259.	3.1	15
36	Investigation of potential interferences in the detection of atmospheric RO <sub><i>x</i></sub> radicals by laser-induced fluorescence under dark conditions. Atmospheric Measurement Techniques, 2016, 9, 1431-1447.	3.1	49

#	Article	IF	CITATIONS
37	A broadband cavity enhanced absorption spectrometer for aircraft measurements of glyoxal, methylglyoxal, nitrous acid, nitrogen dioxide, and water vapor. Atmospheric Measurement Techniques, 2016, 9, 423-440.	3.1	93
38	Twenty years of ambient observations of nitrogen oxides and specified hydrocarbons in air masses dominated by traffic emissions in Germany. Faraday Discussions, 2016, 189, 407-437.	3.2	32
39	Secondary organic aerosol formation from hydroxyl radical oxidation and ozonolysis of monoterpenes. Atmospheric Chemistry and Physics, 2015, 15, 991-1012.	4.9	67
40	Evidence for an unidentified non-photochemical ground-level source of formaldehyde in the Po Valley with potential implications for ozone production. Atmospheric Chemistry and Physics, 2015, 15, 1289-1298.	4.9	36
41	Response to Comment on "Missing gas-phase source of HONO inferred from Zeppelin measurements in the troposphereâ€. Science, 2015, 348, 1326-1326.	12.6	10
42	Intercomparison of Hantzsch and fiber-laser-induced-fluorescence formaldehyde measurements. Atmospheric Measurement Techniques, 2014, 7, 1571-1580.	3.1	24
43	Missing Gas-Phase Source of HONO Inferred from Zeppelin Measurements in the Troposphere. Science, 2014, 344, 292-296.	12.6	154
44	Maximum efficiency in the hydroxyl-radical-based self-cleansing of the troposphere. Nature Geoscience, 2014, 7, 559-563.	12.9	110
45	Parameterization of Thermal Properties of Aging Secondary Organic Aerosol Produced by Photo-Oxidation of Selected Terpene Mixtures. Environmental Science & Technology, 2014, 48, 6168-6176.	10.0	14
46	Suppression of new particle formation from monoterpene oxidation by NO <sub>x</sub> . Atmospheric Chemistry and Physics, 2014, 14, 2789-2804.	4.9	63
47	The balances of mixing ratios and segregation intensity: a case study from the field (ECHO 2003). Atmospheric Chemistry and Physics, 2014, 14, 10333-10362.	4.9	8
48	Atmospheric photochemistry of aromatic hydrocarbons: OH budgets during SAPHIR chamber experiments. Atmospheric Chemistry and Physics, 2014, 14, 6941-6952.	4.9	21
49	Missing SO <sub>2</sub> oxidant in the coastal atmosphere? – observations from high-resolution measurements of OH and atmospheric sulfur compounds. Atmospheric Chemistry and Physics, 2014, 14, 12209-12223.	4.9	38
50	Nighttime observation and chemistry of HO <sub>x</sub> in the Pearl River Delta and Beijing in summer 2006. Atmospheric Chemistry and Physics, 2014, 14, 4979-4999.	4.9	40
51	Modeling of HCHO and CHOCHO at a semi-rural site in southern China during the PRIDE-PRD2006 campaign. Atmospheric Chemistry and Physics, 2014, 14, 12291-12305.	4.9	59
52	OH regeneration from methacrolein oxidation investigated in the atmosphere simulation chamber SAPHIR. Atmospheric Chemistry and Physics, 2014, 14, 7895-7908.	4.9	38
53	Climate and Weather of the Sun-Earth System (CAWSES). Springer Atmospheric Sciences, 2013, , .	0.3	16
54	Experimental evidence for efficient hydroxyl radical regeneration in isoprene oxidation. Nature Geoscience, 2013, 6, 1023-1026.	12.9	132

#	Article	IF	CITATIONS
55	Does the onset of new particle formation occur in the planetary boundary layer?. , 2013, , .		1
56	Stable carbon isotope ratios of toluene in the boundary layer and the lower free troposphere. Atmospheric Chemistry and Physics, 2013, 13, 11059-11071.	4.9	17
57	Missing OH source in a suburban environment near Beijing: observed and modelled OH and HO <sub>2</sub> concentrations in summer 2006. Atmospheric Chemistry and Physics, 2013, 13, 1057-1080.	4.9	188
58	Extending water vapor trend observations over Boulder into the tropopause region: Trend uncertainties and resulting radiative forcing. Journal of Geophysical Research D: Atmospheres, 2013, 118, 11269-11284.	3.3	28
59	Seasonal measurements of OH, NO <i><sub>x</sub></i> , and J(O <sup>1</sup> D) at Mace Head, Ireland. Geophysical Research Letters, 2013, 40, 1659-1663.	4.0	8
60	Intercomparison of NO <sub>3</sub> radical detection instruments in the atmosphere simulation chamber SAPHIR. Atmospheric Measurement Techniques, 2013, 6, 1111-1140.	3.1	49
61	Do Galactic Cosmic Rays Impact the Cirrus Cloud Cover?. Springer Atmospheric Sciences, 2013, , 79-87.	0.3	Ο
62	Comparison of OH concentration measurements by DOAS and LIF during SAPHIR chamber experiments at high OH reactivity and low NO concentration. Atmospheric Measurement Techniques, 2012, 5, 1611-1626.	3.1	75
63	Comparison of N <sub>2</sub> O <sub>5</sub> mixing ratios during NO3Comp 2007 in SAPHIR. Atmospheric Measurement Techniques, 2012, 5, 2763-2777.	3.1	21
64	Exploring the atmospheric chemistry of nitrous acid (HONO) at a rural site in Southern China. Atmospheric Chemistry and Physics, 2012, 12, 1497-1513.	4.9	211
65	Observation and modelling of OH and HO <sub>2</sub> concentrations in the Pearl River Delta 2006: a missing OH source in a VOC rich atmosphere. Atmospheric Chemistry and Physics, 2012, 12, 1541-1569.	4.9	269
66	Comparisons of observed and modeled OH and HO <sub>2</sub> concentrations during the ambient measurement period of the HO <sub>x</sub> Comp field campaign. Atmospheric Chemistry and Physics, 2012, 12, 2567-2585.	4.9	30
67	HO <sub>x</sub> budgets during HOxComp: A case study of HO <sub>x</sub> chemistry under NO <sub>x</sub> â€limited conditions. Journal of Geophysical Research, 2012, 117, .	3.3	38
68	SOA from limonene: role of NO <sub>3</sub> in its generation and degradation. Atmospheric Chemistry and Physics, 2011, 11, 3879-3894.	4.9	123
69	Detection of HO <sub>2</sub> by laser-induced fluorescence: calibration and interferences from RO <sub>2</sub> radicals. Atmospheric Measurement Techniques, 2011, 4, 1209-1225.	3.1	199
70	Atmospheric OH reactivities in the Pearl River Delta – China in summer 2006: measurement and model results. Atmospheric Chemistry and Physics, 2010, 10, 11243-11260.	4.9	231
71	lsotope effect in the formation of H <sub>2</sub> from H <sub>2</sub> CO studied at the atmospheric simulation chamber SAPHIR. Atmospheric Chemistry and Physics, 2010, 10, 5343-5357.	4.9	25
72	Intercomparison of measurements of NO <sub>2</sub> concentrations in the atmosphere simulation chamber SAPHIR during the NO3Comp campaign. Atmospheric Measurement Techniques, 2010, 3, 21-37.	3.1	77

FRANZ ROHRER

#	Article	IF	CITATIONS
73	A correlation study of highâ€altitude and midaltitude clouds and galactic cosmic rays by MIPASâ€Envisat. Journal of Geophysical Research, 2010, 115, .	3.3	8
74	Intercomparison of peroxy radical measurements obtained at atmospheric conditions by laser-induced fluorescence and electron spin resonance spectroscopy. Atmospheric Measurement Techniques, 2009, 2, 55-64.	3.1	30
75	High static stability in the mixing layer above the extratropical tropopause. Journal of Geophysical Research, 2009, 114, .	3.3	44
76	Amplified Trace Gas Removal in the Troposphere. Science, 2009, 324, 1702-1704.	12.6	550
77	lsoprene oxidation by nitrate radical: alkyl nitrate and secondary organic aerosol yields. Atmospheric Chemistry and Physics, 2009, 9, 6685-6703.	4.9	208
78	Statistical analysis of water vapour and ozone in the UT/LS observed during SPURT and MOZAIC. Atmospheric Chemistry and Physics, 2008, 8, 6603-6615.	4.9	30
79	Simulation chamber investigation of the reactions of ozone with shortâ€chained alkenes. Journal of Geophysical Research, 2007, 112, .	3.3	83
80	On the use of nonmethane hydrocarbons for the determination of age spectra in the lower stratosphere. Journal of Geophysical Research, 2007, 112, .	3.3	14
81	Intercomparison of Two Hydroxyl Radical Measurement Techniques at the Atmosphere Simulation Chamber SAPHIR. Journal of Atmospheric Chemistry, 2007, 56, 187-205.	3.2	76
82	Global distribution pattern of anthropogenic nitrogen oxide emissions: Correlation analysis of satellite measurements and model calculations. Journal of Geophysical Research, 2006, 111, .	3.3	44
83	Seasonal variations and profile measurements of photolysis frequenciesj(O1D) andj(NO2) at the ECHO forest field site. Journal of Geophysical Research, 2006, 111, .	3.3	8
84	Simulation chamber studies on the NO3chemistry of atmospheric aldehydes. Geophysical Research Letters, 2006, 33, n/a-n/a.	4.0	24
85	Strong correlation between levels of tropospheric hydroxyl radicals and solar ultraviolet radiation. Nature, 2006, 442, 184-187.	27.8	352
86	Characterisation of the photolytic HONO-source in the atmosphere simulation chamber SAPHIR. Atmospheric Chemistry and Physics, 2005, 5, 2189-2201.	4.9	237
87	Actinometric measurements of NO <sub>2</sub> photolysis frequencies in the atmosphere simulation chamber SAPHIR. Atmospheric Chemistry and Physics, 2005, 5, 493-503.	4.9	82
88	Vertical profiles of HDO/H2O in the troposphere. Journal of Geophysical Research, 2005, 110, .	3.3	40
89	Kinetic Study of the OH-isoprene and O3-isoprene reaction in the atmosphere simulation chamber, SAPHIR. Geophysical Research Letters, 2004, 31, n/a-n/a.	4.0	37
90	On the decay of stratospheric pollutants: Diagnosing the longest-lived eigenmode. Journal of Geophysical Research, 2004, 109, .	3.3	9

FRANZ ROHRER

#	Article	IF	CITATIONS
91	Seasonal variability and trends of volatile organic compounds in the lower polar troposphere. Journal of Geophysical Research, 2003, 108, n/a-n/a.	3.3	33
92	Concentration and stable carbon isotopic composition of ethane and benzene using a global three-dimensional isotope inclusive chemical tracer model. Journal of Geophysical Research, 2003, 108, n/a-n/a.	3.3	18
93	OH in the coastal boundary layer of Crete during MINOS: Measurements and relationship with ozone photolysis. Atmospheric Chemistry and Physics, 2003, 3, 639-649.	4.9	86
94	Tritiated water vapor in the stratosphere: Vertical profiles and residence time. Journal of Geophysical Research, 2002, 107, ACH 8-1.	3.3	27
95	Free Radicals and Fast Photochemistry during BERLIOZ. Journal of Atmospheric Chemistry, 2002, 42, 359-394.	3.2	85
96	Actinic Radiation and Photolysis Processes in the Lower Troposphere: Effect of Clouds and Aerosols. Journal of Atmospheric Chemistry, 2002, 42, 413-441.	3.2	20
97	Free Radicals and Fast Photochemistry during BERLIOZ. , 2002, , 359-394.		20
98	Actinic Radiation and Photolysis Processes in the Lower Troposphere: Effect of Clouds and Aerosols. , 2002, , 413-441.		4
99	Intercomparison of NO2photolysis frequency measurements by actinic flux spectroradiometry and chemical actinometry during JCOM97. Geophysical Research Letters, 2000, 27, 1115-1118.	4.0	32
100	Dependence of the OH concentration on solar UV. Journal of Geophysical Research, 2000, 105, 3565-3571.	3.3	115
101	Title is missing!. Journal of Atmospheric Chemistry, 1998, 31, 119-137.	3.2	42
102	Study of ozone formation and transatlantic transport from biomass burning emissions over West Africa during the airborne Tropospheric Ozone Campaigns TROPOZ I and TROPOZ II. Journal of Geophysical Research, 1998, 103, 19059-19073.	3.3	67
103	On the use of hydrocarbons for the determination of tropospheric OH concentrations. Journal of Geophysical Research, 1998, 103, 18981-18997.	3.3	70
104	Mixing Ratios and Photostationary State of NO and NO2 Observed During the POPCORN Field Campaign at a Rural Site in Germany. , 1998, , 119-137.		3
105	On the significance of regional trace gas distributions as derived from aircraft campaigns in PEM-West A and B. Journal of Geophysical Research, 1997, 102, 28333-28351.	3.3	9
106	Tropospheric mixing ratios of NO obtained during TROPOZ II in the latitude region 67°N-56°S. Journal of Geophysical Research, 1997, 102, 25429-25449.	3.3	15
107	Estimations of global no, emissions and their uncertainties. Atmospheric Environment, 1997, 31, 1735-1749.	4.1	285
108	The passive transport of NOx emissions from aircraft studied with a hierarchy of models. Atmospheric Environment, 1997, 31, 1783-1799.	4.1	18

#	Article	IF	CITATIONS
109	Climatologies of NOxx and NOy: A comparison of data and models. Atmospheric Environment, 1997, 31, 1851-1904.	4.1	111
110	The global tropospheric distribution of NOxestimated by a three-dimensional chemical tracer model. Journal of Geophysical Research, 1996, 101, 18587-18604.	3.3	35
111	Comparison of measured OH concentrations with model calculations. Journal of Geophysical Research, 1994, 99, 16633.	3.3	58
112	Global Measurements of Photochemically Active Compounds. , 1994, , 205-222.		4
113	The Atmospheric Distribution of NO, O3, CO, and CH4 above the North Atlantic Based on the STRATOZ III Flight. , 1993, , 171-187.		1
114	Sources and distribution of NO <sub><i>x</i></sub> in the upper troposphere at northern mid″atitudes. Journal of Geophysical Research, 1992, 97, 3725-3738.	3.3	145
115	Surface NO and NO2 mixing ratios measured between 30� N and 30� S in the Atlantic region. Journal of Atmospheric Chemistry, 1992, 15, 253-267.	3.2	28
116	Electronic quenching of imidogen(c1.Pl.). The Journal of Physical Chemistry, 1989, 93, 7824-7832.	2.9	33
117	Kinetic study of imidogen(a) by emission. The Journal of Physical Chemistry, 1989, 93, 3170-3174.	2.9	35
118	The 193 (and 248) nm photolysis of HN3: Formation and internal energy distributions of the NH (a 1Δ,) Tj ET	QqQ 0 0 r	3BT /Overloc
119	Perturbations in UV Laser Photolysis Experiments: Blast Wave Formation. Zeitschrift Fur Physikalische Chemie, 1988, 158, 131-146.	2.8	3
120	Generation of NH(a 1Δ) in the 193 nm photolysis of ammonia. Journal of Chemical Physics, 1987, 86, 2036-2043.	3.0	54
121	Collisionâ€induced intersystem crossing NH(c 1Î)→NH(A 3Î). Journal of Chemical Physics, 1987, 86, 226	-233.	27
122	Two-photon formation of NH/ND(A3Î) in the 193 nm photolysis of ammonia. I. Mechanism and identification of the intermediate species. Chemical Physics, 1987, 118, 141-152.	1.9	34
123	Hydroxyl(A) production in the 193-nm photolysis of nitrous acid. The Journal of Physical Chemistry, 1986, 90, 2635-2639.	2.9	21
124	Excitation mechanism for hydroxyl(A) in the argon fluoride excimer laser photolysis of nitric acid. The Journal of Physical Chemistry, 1986, 90, 1294-1299.	2.9	33
125	Determination of the excitation mechanism for photofragment emission in the ArF laser photolysis of NH3, N2H4, HNO3 and CH3NH2. Chemical Physics Letters, 1985, 116, 374-379.	2.6	29
126	Intelligent microcomputer interface for continuous registration and storage of spectra by photon counting. Review of Scientific Instruments, 1984, 55, 375-378.	1.3	6

	Fr	Franz Rohrer		
#	Article	IF	CITATIONS	
127	Radiative lifetime of metastable NH(b $1\hat{b}$ +). Chemical Physics Letters, 1984, 107, 347-350.	2.6	28	

NH(all<sup>°</sup> → X3l̂£â<sup>^</sup>) emission from the gas-phase photolysis of HN3. Chemical Physics Letters, 1984, 111, 234-2372.6 39